# COMPUTER SIMULATION STUDIES OF TWO INJECTION OPTIONS FOR 12 GEV CEBAF UPGRADE

Y. Zhang, J. F. Benesch, Y. Chao, J.M. Grames, R. Kazimi, G. A. Krafft, M. Tiefenback, B. C. Yunn

Jefferson Lab, Newport News, VA 23606, USA

*Abstract*

As part of CEBAF 12 GeV energy upgrade, the injection energy needs to be increased from 67 MeV to 123 MeV. Two upgrade options for attaining the desired energy increase are under evaluation: (1) a single-pass straight-through injector by replacing the present injector SRF modules with new and higher gradient modules; (2) a two-pass re-circulated injector in which the electron beam goes through the existing SRF modules twice to achieve the necessary energy gain. In this tech note we present PARMELA simulation studies on these two upgrade options.

## 1. INTRODUCTION

Jefferson Lab is aiming toward a major upgrade of CEBAF accelerator. The maximum machine energy will be increased from 6 GeV to 12 GeV. In order to preserve the existing beam transport line and optics matching, the ratio of the injector energy and energies at experimental halls would be ideally kept the same as the current machine. Thus, the injector energy needs to be increased from 67 MeV presently to 123 MeV. In the baseline design of the CEBAF 12 GeV upgrade, the present 100 keV DC gun and beam formation up to 5 MeV remain unchanged. However, two SRF modules in the current injector cannot provide the required energy increase. There are two upgrade options currently under consideration. The first option is to upgrade two SRF modules to higher gradient ones without changing the present injector configuration. The second option uses the existing injector SRF modules twice via recirculation. The two-pass re-circulating injector is obviously more complicated than the single-pass straight-through injector. Such complication could have impact on beam quality at injection into the CEBAF accelerator. Stability and operability of the injector are also important factors for selection of upgrade options. In this tech note we present a comparative study on the stability of both injector upgrade options by PARMELA simulations.

## 2. UPGRADE OF CEBAF INJECTOR

### *2.1 Current CEBAF Injector*

Figure 1 shows schematic layout of the current CEBAF injector. It can be divided into two parts. The first part, the 5 MeV section, is from the photo cathode to end of the quarter cryo module. It includes a photo cathode DC gun, a pre-buncher, apertures, a chopper, a buncher, a capture and a quarter cryo module. The capture and quarter cryo module accelerate the 100 keV beam from the DC gun to 5MeV at end of this section. The second part of the CEBAF injector is from downstream

of the quarter cryo module to the injection chicane. In this part of the injector, two eight-cavity SRF cryo modules accelerate beams to the injection energy between 23 and 67 MeV. The beam then passes through an injection chicane before joining with the re-circulated high energy beams in the main machine. Magnetic elements (dipoles, quadruples and solenoids) distributed along the injector beam line provide beam steering, transverse focusing as well as the final matching to the main accelerator.

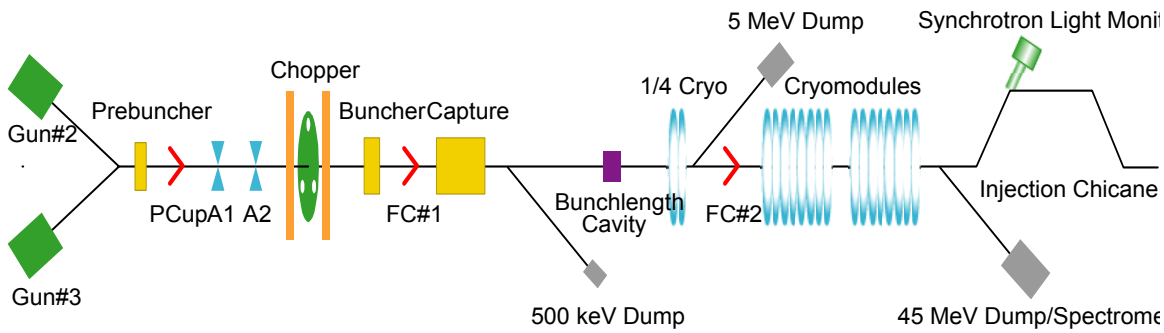


Figure1: Layout of the CEBAF Injector

It should be pointed out that machine setup for the 5 MeV section is independent of the final injection energy in the present machine. When upgrading the injector for 12 GeV CEBAF, this 5 MeV section should remain unchanged. Any changes to the injector configuration for upgrade should be confined in the beam line after the 5 MeV section and before the final injection chicane.

In the current injector, the injection chicane is run with $M_{56}\neq 0$ and the second cryo module is run slightly off crest to produce beam bunching. Because the 12 GeV upgrade does not require such a highly bunched beam, it is not anticipated that bunching in the injection chicane is need and $M_{56}$ will be set to zero. Therefore our calculations will assume the beam pass through the module will be at the crest phase.

### *2.2 Upgrade Option 1: Single Pass straight-through*

This upgrade option requires minimum change of the current CEBAF injector. The existing two cryo modules each consist of eight half-meter SRF cavities with average field gradient of 7.75 MV/m. To achieve 123 MeV injection energy, an average 14.75 MV/m field gradient is needed. This can be realized by refurbishing the first module and replacing the second module by a high gradient one. The field gradients will be 7 MV/m and 8.5 MV/m for the first and second set of four cavities in the first module respectively, and 15.5 MV/m for the second and new module, of which each SRF cavity is 70 cm long. Like the current CEBAF injector, first four cavities of the first cryo module are set at a slightly lower gradient in order to lower the RF focusing effects for the 5 MeV injection beam while still not fully relativistic yet.

### *2.3 Upgrade Option 2: Recirculation*

No upgrade of SRF modules is required in this option. Instead, electron beams will pass through two SRF modules twice to double the energy gain. A compact re-circulating beam line on a horizontal plane will be fitted inside the CEBAF injector underground tunnel to produce the beam recirculation. Figure 2 shows the schematic re-circulating beam line, which would replace the beam line from end of the 5 MeV section to entrance of the injection chicane in Figure 1. The recirculating beam line includes two 180° arcs, a path-length chicane, three more chicanes for

entering/exiting the recirculator and a back leg matching section. The beams coming from the 5 MeV section reaches 64 MeV after the first pass of the two modules on crest phases. It then goes recirculation through two 180° re-circulating arcs, each consisting of four 45° non-sector bends which also provide additional transverse edge focusing. The path length chicane ensures that beam arrives at SRF modules for the second pass on crest phases again. The beam reaches 123 MeV after the second pass and is finally extracted from the recirculator by the exiting chicane. A set of six quads (not shown in Figure 2) after exiting chicane provides intermediate matching for final North Linac injection.

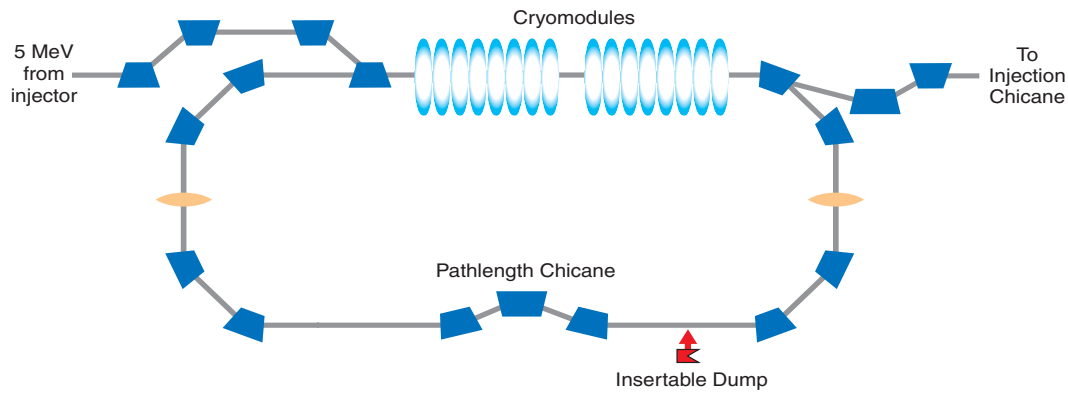


Figure 2: Schematic of the recirculation beam line.

## 3. PARMELA SIMULATIONS

Computer model for the 12 GeV CEBAF re-circulated injector was first built up on an OpitM deck [1]. The OptiM deck for the single-pass straight-through injector is identical to the present CEBAF injector deck with a new energy boost plan. Both OptiM desks start at end of the 5 MeV section and with a set of assumed initial conditions (emittances, Twiss parameters and energy spread) of the beam. Being a 4D matrix mapping software tool, the OptiM decks allow one to design injector beam lines and adjust their transverse optics very efficiently. Nominal parameter settings were obtained by considering the geometric constraints of the tunnel and the transverse optics. The OptiM decks then were translated into PARMELA decks for full-scale macro-particle based simulations. The JLab version PARMELA code is based on an earlier version of the LANL PARMELA software and had been extensively extended and customized for the CEBAF injector. PARMELA simulations not only can validate the OptiM injector models but also include additional longitudinal motion and space charge effect in computer modeling.

PARMELA simulations in this study were performed for the whole CEBAF injector. The first part of simulations, the 5 MeV section (from the photo-cathode to the quarter cryo module), was adopted from an existing PARMELA model which has been improved and experimentally validated recently [2]. Simulations on the second injector part were continued from simulations of the first part. All simulations were done for a 100 μA CW electron beam at 499 MHz frequency and the initial distribution of the electron bunch at the photocathode is assumed multidimensional Gaussian in phase space with parameters derived from the Ti-sapphire laser beam of the electron DC gun. 2000 micro particles were used in all simulation runs.

# 4. CASES OF NOMINAL SETTINGS

As pointed out in the previous section, macro-particle phase space distribution at end of the 5 MeV part simulations was used as initial conditions for the next injector part PARMELA simulations. Since Twiss parameters and emittances at 5 MeV from PARMELA simulations are different from the initial conditions used in the original OptiM deck of reference 1, quad field gradients in the recirculated injector had been adjusted in order to match the beam. Similarly, in the straight-through injector, quad settings had also been adjusted from the current CEBAF machine settings in order to accommodate higher injection energy. Table 1 and 2 list the quad field gradients for both injectors.

Table 1. Quad nominal setting in the single-pass straight-through injector

| Name | MQJ0L01 | MQJ0L01A | MQJ0L02 | MQJ0L02A | MQJ0L03A | MQJ0L03 | MQJ0L04 |
|---|---|---|---|---|---|---|---|
| G [kG/cm] | 3.6 | -7.3 | 9 | -5.2 | 8.0 | -7.1 | 6.4 |
| Name | MQJ0L05 | MQD0L06 | MQD0L07 | MQD0L08 | MQD0L09 | MQD0L10 | |
| G [kG/cm] | 20 | 65 | -40 | 50 | -40 | 50 | |

Table 2. Quad nominal setting in the two-pass recirculated injector

| Name | MQZ1 | MQZ2 | MQZ3 | MOZ4 | MQZ5 | MQZ6 | MQA3 | MQA5 | MQJ0L05 | MQX1 |
|---|---|---|---|---|---|---|---|---|---|---|
| G [kG/cm] | 7.49 | -13.63 | 16.81 | -17.04 | 16.23 | -6.82 | 0.32 | -1.79 | 0 | -7.59 |
| Name | MQB2 | MQM0 | MQM1 | MQM2 | MQM3 | MQM31 | MQC3 | MQM4 | MQM5 | MQM6 |
| G [kG/cm] | 251.1 | 16.61 | -51.24 | 78.89 | -82.66 | 12.65 | 36.88 | -23.93 | 9.10 | -34.3 |
| Name | MQB5 | MQD1 | MQD3 | MQE1 | MQE2 | MQIC1 | MQIC2 | MQIC3 | MQIC4 | |
| G [kG/cm] | 251.1 | -11.72 | 0.049 | -29.7 | -9.05 | -257.3 | 7.52 | 3.81 | -85.19 | |

Figure 3 and 4 show the RMS bunch length and transverse size along the beam line for the single-pass straight-through and the two-pass recirculated injector respectively by PARMELA simulations. The vertical lines in these plots mark the end of the 5 MeV section and beginning of the upgraded section of the injector. These plots show that bunch length of the beam is already below its design value at 5 MeV before entering the two accelerating SRF modules. They also show that bunch lengths remain very small for both injectors during the next stage of accelerating to 123 MeV. For the transverse motion, both horizontal and vertical sizes are confined below 0.5 mm after passing of two SRF modules in the straight-through injector or after first passing of two SRF modules in the recirculated injector. There is no particle loss in the beam transport through the whole injector of both upgrade options. The increase of the horizontal size right after the 5 MeV section for the recirculated injector is due to large dispersion of the dipole moments in the 5 MeV chicane. Table 3 summarizes beam properties at end of simulated beam lines (before the injector chicane) for both injectors. Emittances and bunch length of the recirculator injectors are a factor of two large than the straight-through injector.

Table 3. Beam properties at 5 MeV and at 123 MeV

| | Energy (E) | Bunch length ($\sigma_z$) | Horizontal Size ($\sigma_x$) | Vertical size ($\sigma_y$) | $\beta_x$ | $\beta_y$ | $\alpha_x$ | $\alpha_y$ | Horizontal emittance ($\varepsilon_x$) | Vertical emittance ($\varepsilon_y$) | Energy spread ($\delta E/E$) |
|---|---|---|---|---|---|---|---|---|---|---|---|
| | MeV | mm | mm | mm | M | M | | | pi mm mrad | pi mm mrad | $10^{-4}$ |
| At 5 MeV | 5.55 | 0.55 | 0.54 | 0.56 | 5.7 | 14 | -0.8 | -1.5 | 0.59 | 0.27 | 32 |
| Single-pass | 123.5 | 0.24 | 0.18 | 0.03 | 15 | 1 | 1.2 | 1.1 | 0.53 | 0.27 | 1.3 |
| Two-pass | 123.5 | 0.20 | 0.51 | 0.06 | 61 | 0.9 | -20 | 0.1 | 1.03 | 0.98 | 2.9 |

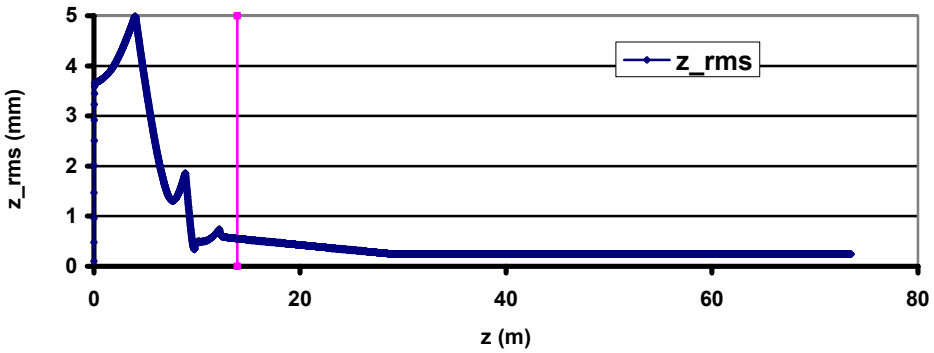


Figure 3a. RMS bunch length for a single-pass straight-through CEABF injector

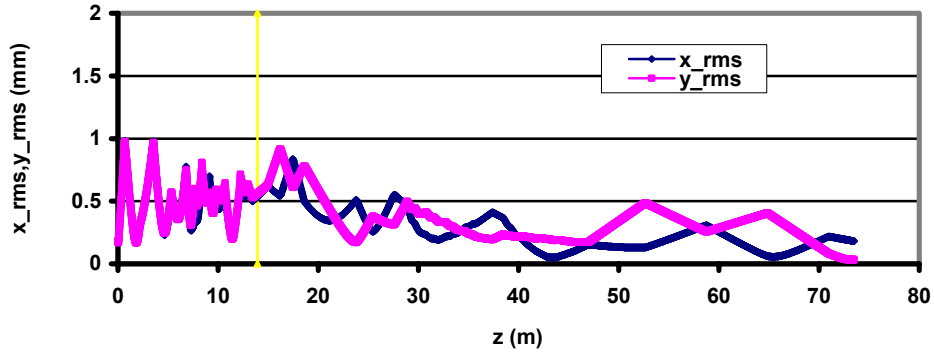


Figure 3b. RMS transverse sizes for a single-pass straight-through CEABF injector

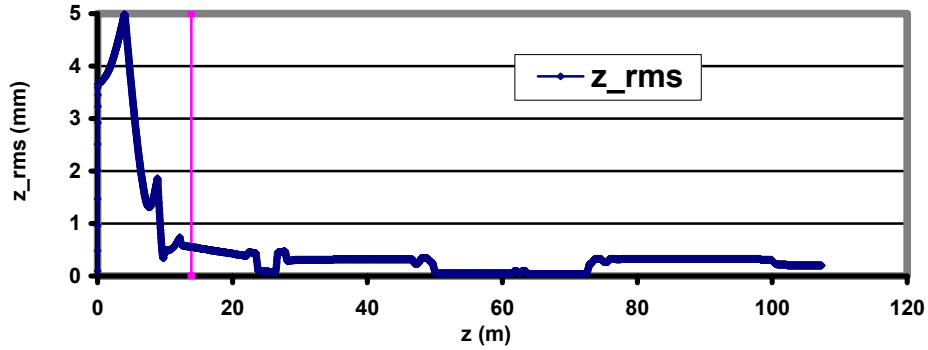


Figure 4a. RMS bunch length for a two-pass recirculated CEBAF injector

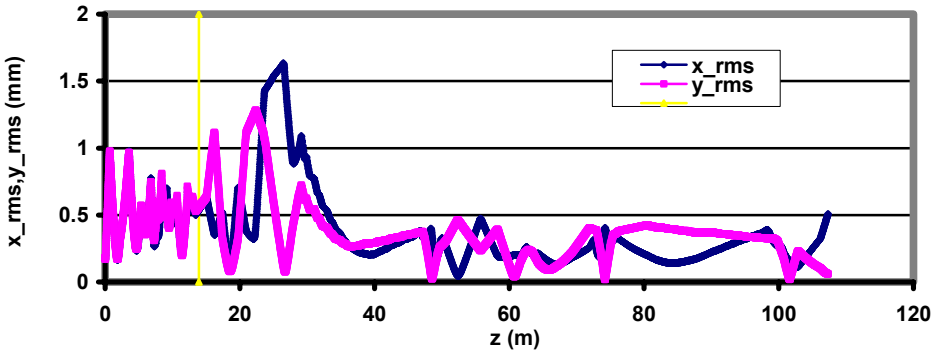


Figure 4b. RMS transverse for a two-pass recirculated CEBAF injector

## 5. SENSITIVITY STUDIES

Beam line stability is an important condition of a good injector. Small deviations from an injector setting should not disrupt beam formation and transport very much. This insensitivity of parameters should lead to a desired high reliability and operability of the injector. We performed a series of PARMELA simulations to explore parameter sensitivity for both options of injector upgrade. In each simulated case, only one injector parameter was varied by a small amount from its nominal value while other parameters were kept unchanged to model small perturbations in machine operation. Such perturbations arise from various reasons and conditions, including imperfect magnetic or RF elements, imperfect element alignment, uncontrolled fluctuations, mechanical, electric or thermal disturbances, etc. The following is a list of cases being simulated

1. Energy deviation at 5 MeV: the beam energy is 30 keV (0.6%) higher than the nominal case at end of the 5 MeV section;
2. Energy deviation at 5 MeV: the beam energy is 30 keV (-0.6%) lower than the nominal case at end of the 5 MeV section;
3. Phase deviation at 5 MeV: 1° RF phase advance at end of 5 MeV section;
4. Phase deviation at 5 meV: 1° RF phase delay at end of 5 MeV section;
5. Path length deviation: 0.5 mm increase of the path length for the single-pass option and 1 mm increase for the two-pass option, distributed at 2 or 4 locations with 0.25 mm increments alone the beam line respectively;
6. Laser pulse deviation: 10% increase of pulse length of the DC gun driving laser, which induces a 10% increase in the initial bunch length at the photo-cathode;
7. Laser spot size deviation: 10% increase of spot size of the DC gun driving laser, which induces a 10% increase of the initial beam size as well as initial emitance at the photo-cathode;
8. Magnetic lens deviation: 1% random errors of focusing lengths of all solenoids in the 5 MeV section, such changes will effect the beam size but not emittance at end of the 5 MeV section;
9. Magnetic quad deviation: 1% random change to quad field gradients after the 5 MeV section, this includes the quads in the recirculation line for the two-pass injector.

The first four cases deal with the sensitivity of RF phase and amplitudes at 5 MeV. These errors will effect phases (and arriving times) of the accelerating SRF modules. The fifth case models the path length expansion due to temperature fluctuations. Case 6 and 7 test sensitivity of the injectors to the driving laser of the DC gun. The last two cases explore stability of beam optics, i.e., sensitivity of the small fluctuations of electric currents of lenses or quads.

For all simulated cases, it is found that the beam transport through the whole injector remains at 100%. Figure 5 (a-c) are transverse sizes and bunch length of all simulated cases for the single-pass injector. These plots clearly indicate that the single-pass straight-through injector has very high stability on its beam line. Transverse sizes and bunch length shown in Figures 6 (a-c) display, in general, more complicated behaviors in the two-pass recirculated injector. There are two highly notable features: large spikes of the horizontal RMS size at several strong bending regions (180° bends and chicanes), and sudden large jumps of the bunch lengths at same bending regions. They are both related to high dispersions in the strong bending region. Table 4 summaries the beam properties (sizes, bunch length, emittances and energy spread) at end of simulations (before the injection chicane) for two injectors. The final beam properties of the single-pass injector in all simulated cases are very closed to the nominal case. For the recirculated injector, results are quite mixed. On one hand, the injector has equally good stability on transverse optics even there are large horizontal dispersions in several strong bending regions. It also shows good tolerance to perturbations on the DC gun driving laser. On the other hand, with huge changes of the bunch

length and energy spread on the first 5 cases (as highlighted in yellow color in Table 4), the injector clearly are very sensitive to energy and phase changes at 5 MeV and small path length changes.

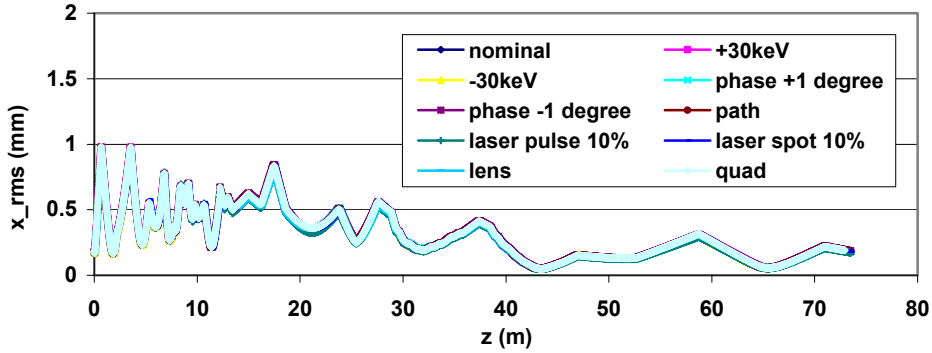


Figure 5a. Horizontal RMS size for a single-pass straight-through injector

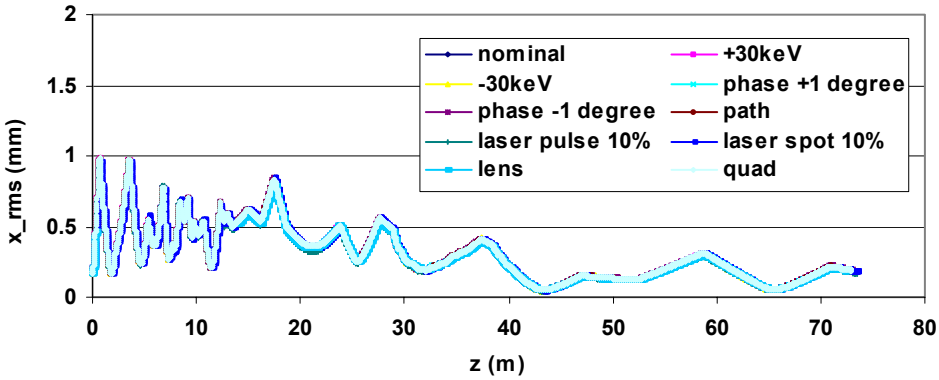


Figure 5b. Vertical RMS size for a single-pass straight-through injector

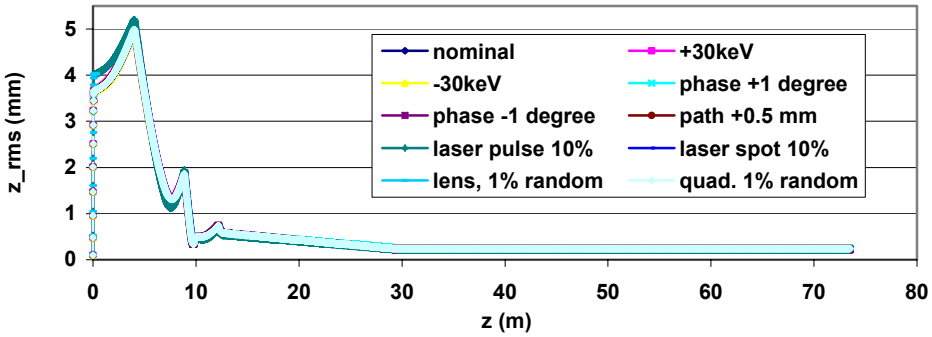


Figure 5c. RMS bunch length for a single-pass straight-through injector

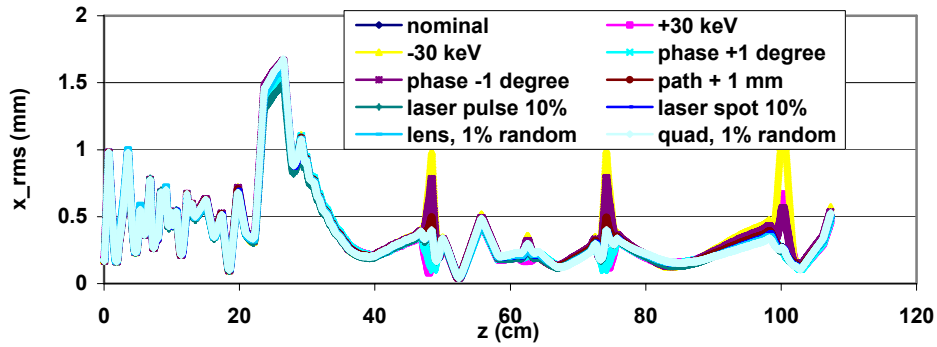


Figure 6a. Horizontal RMS size for a two-pass recirculated injector

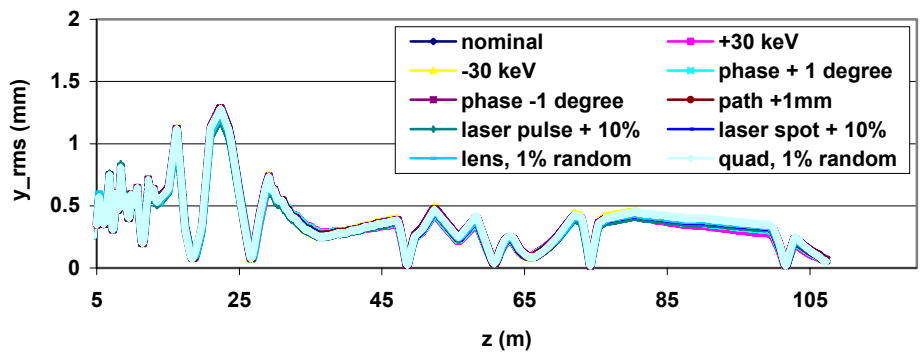


Figure 6b. Vertical RMS size for a two-pass recirculated injector

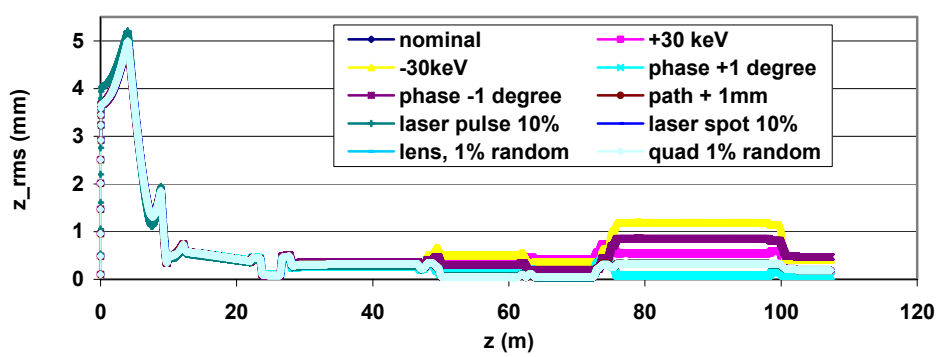


Figure 6c. RMS bunch length for a two-pass recirculated injector

Table 4. Sensitivity of bunch length and energy spread to deviations from nominal

| | One-pass Straight-through Option | | | | | | Two-pass Recirculation Option | | | | | |
|---|---|---|---|---|---|---|---|---|---|---|---|---|
| | $\sigma_x$ | $\sigma_y$ | $\varepsilon_x$ | $\varepsilon_y$ | $\sigma_z$ | $\delta E/E$ | $\sigma_x$ | $\sigma_y$ | $\varepsilon_x$ | $\varepsilon_y$ | $\sigma z$ | $\Delta E/E$ |
| | mm | mm | pi mm mrad | pi mm mrad | mm | $10^{-4}$ | mm | mm | pi mm mrad | pi mm mrad | mm | $10^{-4}$ |
| **Nominal** | **0.18** | **0.034** | **0.53** | **0.27** | **0.24** | **1.3** | **0.51** | **0.060** | **1.03** | **0.98** | **0.2** | **2.9** |
| +30 keV at 5 MeV | 0.17 | 0.034 | 0.53 | 0.27 | 0.24 | 2.6 | 0.47 | 0.067 | 0.97 | 0.97 | 0.16 | 8.3 |
| -30 keV at 5 MeV | 0.18 | 0.034 | 0.52 | 0.27 | 0.23 | 0.5 | 0.57 | 0.065 | 1.16 | 1.07 | 0.4 | 19.6 |
| Path + 0.5mm or 1mm | 0.18 | 0.034 | 0.53 | 0.27 | 0.24 | 0.5 | 0.51 | 0.06 | 10.4 | 0.98 | 0.41 | 1.6 |
| Phase + 1° | 0.18 | 0.034 | 0.52 | 0.27 | 0.25 | 1.9 | 0.49 | 0.062 | 1.01 | 0.97 | 0.07 | 0.6 |
| Phase - 1° | 0.18 | 0.034 | 0.53 | 0.27 | 0.22 | 0.79 | 0.54 | 0.061 | 1.08 | 1.01 | 0.47 | 9.1 |
| Laser pulse 10% increase | 0.17 | 0.034 | 0.46 | 0.27 | 0.22 | 1.2 | 0.49 | 0.054 | 0.91 | 0.86 | 0.19 | 3.1 |
| Laser spot 10% increase | 0.18 | 0.034 | 0.52 | 0.27 | 0.24 | 1.3 | 0.50 | 0.060 | 0.99 | 0.94 | 0.19 | 2.9 |
| Solenoid 1% random change | 0.18 | 0.034 | 0.51 | 0.27 | 0.23 | 1.3 | 0.50 | 0.058 | 0.97 | 0.94 | 0.19 | 2.8 |
| Quad 1% random change | 0.18 | 0.036 | 0.53 | 0.27 | 0.24 | 1.3 | 0.53 | 0.053 | 0.99 | 0.97 | 0.19 | 2.9 |

## 6. DISPERSION

The high sensitivity of bunch length and energy spread on beam energy, RF phases and path length changes for the recirculated injector is due to the fact that the 180-degree bends in the recirculated beam line are not isochronous. As shown in Table 5, M56 for each 180-degree bend is about 113 cm. A beam with a slightly higher/lower energy (in case 1 and 2) or with a slight RF phase error (in case 3, 4 and 5) would arrive the two SRF modules slightly off crest phases. Then the energy spread of the beam would be amplified at off-crest passing of the SRF modules. A large energy spread multiplied by a large M56 will change the bunch length significantly in the 180-degree bends. As a result, the large bunch length would amplify energy spread in the next high dispersion element groups. In such cycle, the beam energy, RF phase, bunch length and energy spread all couple together and continue to amplify one another. A large M56 creates a large dependency of beam timing through the SRF cavities on energy fluctuations. That in turn contributes to fluctuations in the final bunch length. Since the nominal bunch length is small, about 0.2 mm, therefore even small changes to its value are significant, as shown in Figure 6c.

Table 5. M56 and energy spread in the recirculated injector

| | 1st chicane | 1st 180° bend | Path length chicane | 2nd 180° bend | 2nd chicane | 3rd chicane |
|---|---|---|---|---|---|---|
| M56 (cm) | 23.03 | -112.7 | 16.9 | -112.8 | 0.0754 | 47.2 |
| | | | | | | |
| | DE/E ($10^{-4}$) | DE/E ($10^{-4}$) | DE/E ($10^{-4}$) | DE/E ($10^{-4}$) | DE/E ($10^{-4}$) | DE/E ($10^{-4}$) |
| Nominal | 31.1 | 3.1 | 3.1 | 3.1 | 3.1 | 2.9 |
| E+30 keV | 31.2 | 1.2 | 1.2 | 1.2 | 1.2 | 8.3 |
| E-30keV | 30.9 | 7.4 | 7.4 | 7.4 | 7.4 | 19.6 |
| RF phase + 1 degree | 29.6 | 1.1 | 1.1 | 1.1 | 1.1 | 0.7 |
| RF phase – 1 degree | 32.6 | 5.9 | 5.9 | 5.9 | 5.9 | 9.1 |
| Path length + 1mm | 31.1 | 3.8 | 3.8 | 3.7 | 3.7 | 1.6 |
| Laser pulse +10% | 28.2 | 2.9 | 2.9 | 2.9 | 2.9 | 3.1 |
| Laser spot + 10% | 30.7 | 3.1 | 3.0 | 3.1 | 3.1 | 2.9 |
| Solenoid +/-1% random | 30.7 | 3.1 | 3.0 | 3.1 | 3.1 | 2.9 |
| Quad +/-1% random | 31.1 | 3.1 | 3.0 | 3.1 | 3.1 | 2.8 |

## CONCLUSION

We have compared two upgrade options for 12 GeV CEBAF injector using computer modeling. The single-pass straight-through injector performed very much the same as the existing lower energy CEBAF injector. The two-pass re-circulated injector was more complicated but the final beam parameters for a nominal setting were within specifications. Injector sensitivity studies showed that for the recirculated injector, the final bunch length and energy spread are significantly more sensitive to drifts in RF phase and amplitude or path length. This was a consequence of a large M56 in the re-circulation line.

## ACKNOWLEDGEMENT

We would like to thank David Douglas and Eduard Pozdeyev for helpful discussions, and Kevin Beard for PARMELA simulation supports.

## REFERENCES

[1] Y. Chao, JLAB-TN-05-003
[2] Y. Zhang, et. al, Proceeding of EPAC 2004